Journal of Molecular Modeling (2021) 27: 121
https://doi.org/10.1007/s00894-021-04726-z

ORIGINAL PAPER

Substitution effects on novel bicyclo[2.2.1]hepta-7-silylenes by DFT

Nastaran Abedini [1] · Mohamad Z. Kassaee [1]

Received: 7 January 2021 / Accepted: 14 March 2021 / Published online: 6 April 2021

Abstract

Substitution effects on stability ($\Delta E_{s\text{-}t}$) of novel singlet and triplet forms of bicyclo[2.2.1]hepta-7-silylenes are compared and contrasted, at B3LYP/6–311++G** level of theory. All species appear as ground state minima on their energy surface, for showing no negative force constant. Singlets (**1**$_s$-**24**$_s$) are ground state and more stable than their corresponding triplets (**1**$_t$-**24**$_t$). The most stable scrutinized silylenes appear to be 2,3-disilabicyclo[2.2.1]hepta-7-silylene (**9**) for showing the highest value of $\Delta E_{s\text{-}t}$. This stability can be related to our imposed topology and β-silicon effect. The band gaps ($\Delta E_{HOMO–LUMO}$) show the same trend as $\Delta E_{s\text{-}t}$ and the lowest unoccupied molecular orbital energies. Also, the electrophilicity appears inverse correlation with our results of $\Delta E_{s–t}$. The purpose of the present work was to assess the influence of 1 to 6 silicon substitutions on the stability, band gaps, nucleophilicity, electrophilicity, and proton affinity. Finally, our investigation introduces novel silylenes with possible applications in chemistry such as semiconductors, cumulated multidentate ligands, etc.

Keywords Silylene · Stability · DFT · Divalent · Proton affinity

Introduction

Sextet divalent silylenes, with R_1-S̈i-R_2 formula, are of great interest because of evolving from exotic reaction intermediates to important chemical species [1–5]. In contrast to the carbon atom, silylenes have a low ability to form hybrid orbitals [4, 6–9] and therefore prefer the $(ns)^2(np)^2$ valence electron configurations in their divalent species. Since two electrons remain as a singlet pair in the ns orbital, they mostly prefer to exist as singlets and can interact as a Lewis acid or base. Also, the simplest silylene is S̈iH_2, a singlet. The basicity of silylenes may be triggered by their nucleophilicity or proton affinity [4, 10–12]. As a result, they can serve as ancillary ligands in transition metal complexes in which there are synergic electron transfers between the low valent silicon atoms and transition metals such as rhodium [13]. The first heavy alkene (DS̈iCH $(SiMe_3)_2$) was reported in 1976 by Lappert [14]. Silylenes are applied in light-emitting diode (LED), electroluminescence (EL), silicon chemical vapor deposition (CVD) processes, photonics, optics, electronics, and semiconductor [15–23].

Electropositive Si atoms substitution can diminish $\Delta E_{s\text{-}t}$ by lowering the energy of the triplet state [24–26]. Various investigations on silylenes with substituted electropositive atoms were reported [15, 27], such as Apeloig that studied the effects of electropositive substituents on $\Delta E_{s\text{-}t}$ of silylenes [28–31].

Considering the applications of silylenes [15–23, 28], the purpose of the present work is to reach novel silylenes that accommodate up to six electropositive Si atoms at different possible positions (Table 1) and assess the influences of them on the geometrical parameters, stability ($\Delta E_{s\text{-}t}$), the heat of hydrogenation (ΔE_H), nucleophilicity (N), and electrophilicity (ω), at B3LYP/6–311++G** level of theory. Evidently, a number of them can be employed as multidentate ligands.

Computational methods

Full geometry optimizations are accomplished without any symmetry constraints by means of hybrid functional B3LYP [32–35] and the standardized 6–311++G** basis set, by using the GAMESS package of programs [32, 36]. Restricted and unrestricted B3LYP density functional methods are employed for singlet and triplet states, respectively.

✉ Mohamad Z. Kassaee
kassaeem@modares.ac.ir

[1] Chemistry Department, Tarbiat Modares University, Tehran 14115-175, Iran

The nucleophilicity index, N, is defined as $N = E_{HOMO(Nu)} - E_{HOMO(TCNE)}$, where TCNE is tetracyanoethylene and is chosen as the reference [37]. The global electrophilicity, ω [38], is also calculated following the expression $\omega = (\mu^2/2\eta)$, where μ is the chemical potential ($\mu \approx (E_{HOMO} + E_{LUMO})/2$) and η is the chemical hardness ($\eta = E_{LUMO} - E_{HOMO}$) [39] and natural bond orbital (NBO) charges are provided, at the same level of theory [32]. Structural parameters including bond distances, bond angles, dihedral angles, and symmetries are also calculated.

Results and discussion

Silicon substitution effects on thermodynamic and structural parameters of bicyclo[2.2.1]hepta-7-silylenes are compared and contrasted, at B3LYP/6–311++G** level of theory. Special consideration is paid to their singlet (s) and triplet (t) multiplicity, geometrical parameters, relative stability ($\Delta E_{s-t} = E_t - E_s$), nucleophilicity ($N$), electrophilicity ($\omega$), proton affinity ($\Delta E_{PA}$), second-order perturbation stabilization energies ($E^{(2)}$), and band gap ($\Delta E_{HOMO-LUMO}$) (Tables 1, 2, 3, 4, 5, and 6). All structures appear with C_1 symmetry, except silylenes **1**, **4**, **8**, **16**, **21**, and **24** for showing C_2 symmetries.

The silylene bond lengths (A-S̈i or S̈i-D) for $\mathbf{1_s}$–$\mathbf{24_s}$ vs. $\mathbf{1_t}$–$\mathbf{24_t}$ vary in a range of 1.91 A to 2.50 A. Divalents with silicon adjacent to the silylene center have higher S̈i–Si bond lengths than S̈i–C. For instance, the S̈i–Si bond length in silylene $\mathbf{2_s}$ is 0.43 Å longer than S̈i–C. Interestingly, silylenes $\mathbf{10_s}$ and $\mathbf{19_s}$ have the lowest and highest bond lengths. Also, the bond lengths of singlet and triplet silylenes **8**, **9**, and **21** are similar (Table 1).

Divalent bond angles (∠AS̈iD) of our silylenes range from 71.62° to 102.08°. Silylene $\mathbf{4_s}$ with high bond lengths (A–S̈i and S̈i–D = 2.48 Å) has the lowest ∠AS̈iD (71.62°), and $\mathbf{21_t}$ with low bond lengths (A–S̈i and S̈i–D = 1.93 Å) has the highest ∠AS̈iD (102.08°). Triplet silylenes have wider divalent bond angles (∠AS̈iD) than their corresponding singlet states. For example, the ∠AS̈iD in silylene $\mathbf{6_t}$ is 4.74° wider than divalent bond angles $\mathbf{6_s}$. Also, the bond angles (∠S̈iDE and ∠S̈iAF) of singlet silylenes are wider than corresponding triplets. For instance, ∠S̈iDE bond angles of $\mathbf{4_s}$ and $\mathbf{4_t}$ are 103.12° and 98.76°, respectively (Table 1).

The singlet-triplet energy gaps (ΔE_{s-t}) are employed to compare the relative stabilities at B3LYP/6–311++G** levels of theory. The calculation of ΔE_{s-t} in substitution of silicon atoms has been useful in providing insight into how the singlet

Table 1 Optimized bond length (Å), bond angle (∠AS̈id, ∠S̈iDE, and ∠S̈iAF /deg), and symmetry for novel singlet ($\mathbf{1_s}$–$\mathbf{24_s}$) and triplet ($\mathbf{1_t}$–$\mathbf{24_t}$) silylenes, at B3LYP/6–311++G** level

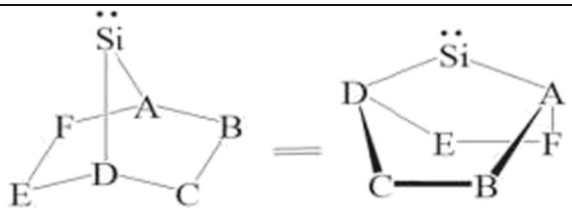

Structures	Silylenes	Symmetry	Bond length (Å)		Bond angle (deg)		
			A-S̈i	S̈i-D	∠AS̈iD	∠S̈iDE	∠S̈iAF
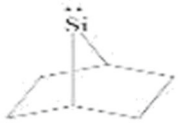	$\mathbf{1_s}$	C_2	1.94	1.94	79.22	101.70	101.70
	$\mathbf{1_t}$	C_2	1.95	1.95	82.13	99.55	99.55
	$\mathbf{2_s}$	C_1	2.40	1.97	75.19	108.09	94.20
	$\mathbf{2_t}$	C_1	2.35	1.96	79.17	106.08	92.08
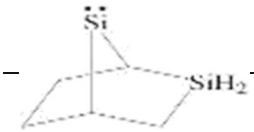	$\mathbf{3_s}$	C_1	1.92	1.95	83.30	102.89	103.70

Table 1 (continued)

	$\mathbf{3}_t$	C_1	1.93	1.95	86.90	98.76	99.79
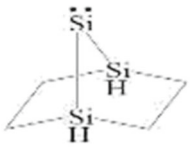	$\mathbf{4}_s$	C_2	2.48	2.48	71.62	103.12	99.04
	$\mathbf{4}_t$	C_2	2.36	2.36	78.95	98.72	97.71
	$\mathbf{5}_s$	C_1	2.39	1.97	80.05	110.44	97.03
	$\mathbf{5}_t$	C_1	2.35	1.95	84.95	104.93	91.98
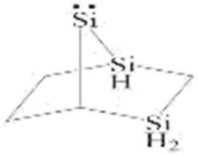	$\mathbf{6}_s$	C_1	2.42	1.93	78.51	110.26	95.57
	$\mathbf{6}_t$	C_1	2.36	1.94	83.25	105.97	91.26
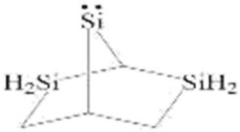	$\mathbf{7}_s$	C_1	1.91	1.97	87.80	105.87	101.60
	$\mathbf{7}_t$	C_1	1.93	1.97	92.08	102.76	97.22
	$\mathbf{8}_s$	C_2	1.94	1.94	88.04	105.81	101.18
	$\mathbf{8}_t$	C_2	1.94	1.94	92.23	104.16	96.35
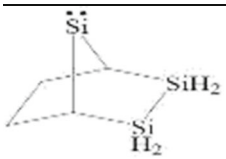	$\mathbf{9}_s$	C_1	1.93	1.93	86.23	105.55	105.57
	$\mathbf{9}_t$	C_1	1.93	1.93	91.05	99.95	99.95
	$\mathbf{10}_s$	C_1	1.91	2.50	81.42	98.89	107.92
	$\mathbf{10}_t$	C_1	1.93	2.37	87.70	96.54	102.88
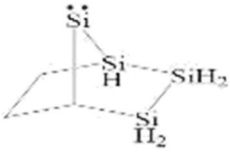	$\mathbf{11}_s$	C_1	2.41	1.93	82.06	111.92	97.76
	$\mathbf{11}_t$	C_1	2.35	1.94	87.98	105.16	91.92
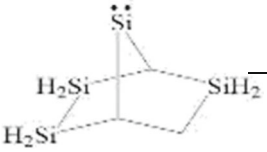	$\mathbf{12}_s$	C_1	1.92	1.94	91.38	104.86	104.81
	$\mathbf{12}_t$	C_1	1.93	1.94	96.87	99.74	100.87
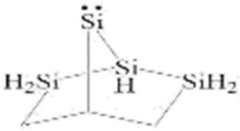	$\mathbf{13}_s$	C_1	2.39	1.97	85.94	110.83	92.47
	$\mathbf{13}_t$	C_1	2.35	1.95	91.78	108.02	88.00

Table 1 (continued)

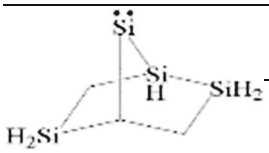	**14**$_s$	C_1	2.42	1.94	83.87	107.78	100.33
	14$_t$	C_1	2.36	1.94	89.39	102.16	97.54
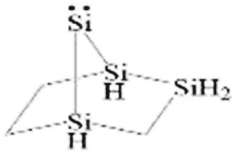	**15**$_s$	C_1	2.39	2.49	76.06	104.94	104.39
	15$_t$	C_1	2.35	2.36	83.27	98.55	97.10
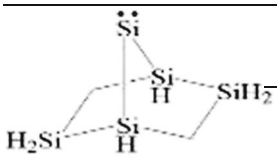	**16**$_s$	C_2	2.48	2.48	79.42	98.54	105.92
	16$_t$	C_2	2.36	2.36	88.18	93.02	103.99
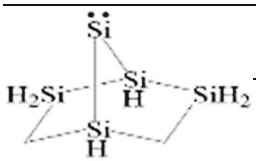	**17**$_s$	C_1	2.37	2.51	80.71	105.59	100.34
	17$_t$	C_1	2.35	2.37	88.72	102.53	93.95
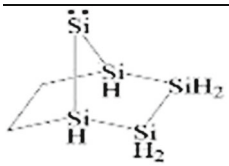	**18**$_s$	C_1	2.40	2.41	79.43	103.92	108.67
	18$_t$	C_1	2.35	2.36	86.79	95.76	99.63
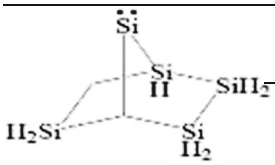	**19**$_s$	C_1	2.50	1.91	85.62	110.02	99.16
	19$_t$	C_1	2.37	1.93	92.96	103.27	96.83
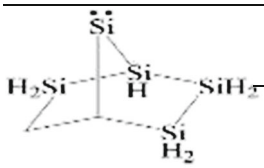	**20**$_s$	C_1	2.41	1.94	88.46	114.02	93.90
	20$_t$	C_1	2.36	1.94	95.28	109.24	87.55
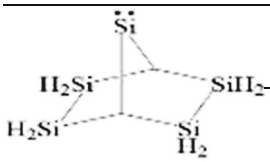	**21**$_s$	C_2	1.93	1.93	85.27	106.70	106.44
	21$_t$	C_2	1.93	1.93	102.08	101.57	101.44
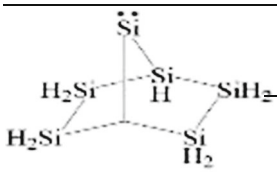	**22**$_s$	C_1	2.49	1.91	90.65	111.62	98.20
	22$_t$	C_1	2.37	1.93	99.31	106.42	93.30
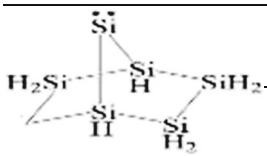	**23**$_s$	C_1	2.39	2.49	83.73	106.46	103.46
	23$_t$	C_1	2.35	2.36	92.81	102.96	93.71

Table 1 (continued)

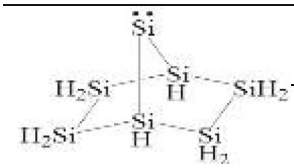	**24$_s$**	C_2	2.41	2.41	88.33	103.64	106.71
	24$_t$	C_2	2.36	2.36	97.84	99.26	99.42

is stabilized (or destabilized) relative to the triplet and also how the geometry of the two states is affected by substitution. All calculated $\Delta E_{s\text{-}t}$ parameters appear with positive values indicating that every singlet silylene is more stable than its corresponding triplet state. For example, singlet **2**$_s$ is 23.40 kcal/mol more stable than its corresponding triplet **2**$_t$. Evidently, among silylenes (**1**$_s$–**24**$_s$), the most stable appears to be singlet **9**$_s$ which is 39.75 kcal/mol more stable than its corresponding triplet **9**$_t$. The overall stability order of our silylenes based on their $\Delta E_{s\text{-}t}$ values is **9** > **1** > **7** > **3** > **21** > **12** > **8** > **2** > **6** > **10** > **5** > **11** > **19** > **22** > **20** > **14** > **4** > **15** > **18** > **17** > **23** > **24** > **16** > **13** (Tables 2). This stability can be related to our imposed topology.

In the case of singlet silylene, we have β-silicon effect [40–43] that the maximum stabilization is a result of the interaction between the β-silicon and anti-bonding character of lone pair (LP*) silylene that increases the electron population of silylene center. This effect is much smaller than the back-donating ability that must be related to both the greater polarizability of the C–Si electron density and to the ability of the C–Si bond to overlap effectively with the LP* on the silylene center. So, silylenes **3**, **7**, **8**, **9**, **12**, and **21** with β-silicon and $\sigma_{C\text{-}Si} \rightarrow LP^*_{Si}$ interactions have higher stability than others. Among them, every silylene that shows the higher level of $E^{(2)}$ for $\sigma_{C\text{-}Si} \rightarrow LP^*_{Si}$ interactions has higher stability than others. So, silylene **9** has the highest stability for two interactions ($\sigma_{C(A)\text{-}Si(B) \text{ and } Si(C)\text{-}C(D)} \rightarrow LP^*_{Si}$) with the highest $E^{(2)}$ (5.23 kcal/mol). Silylene **7** with two interactions ($\sigma_{C(A)\text{-}Si(B) \text{ and } A(C)\text{-}Si(F)} \rightarrow LP^*_{Si}$, $E^{(2)}$ = 4.36 kcal/mol) has higher stability than **3** with one $\sigma_{C(A)\text{-}Si(B)} \rightarrow LP^*_{Si}$ interaction ($E^{(2)}$ = 5.16 kcal/mol). In the same way, silylene **12** despite high $E^{(2)}$ (3.52 kcal/mol) has lower stability than **21**. Because, silylene **12** and **21** have three and four $\sigma_{C(A)\text{-}Si(B)} \rightarrow LP^*_{Si}$ interactions, respectively (Table 3).

As the addition of silicon atoms, their stability decreased. For example, silylene **2** without any interactions has higher

Table 2 Singlet–triplet energy gaps ($\Delta E_{s\text{–}t}$, kcal/mol) for singlet (**1**$_s$–**24**$_s$) and triplet (**1**$_t$–**24**$_t$) silylenes, at B3LYP/6–311++G** level of theory

Silylenes	$\Delta E_{s\text{–}t}$	Silylenes	$\Delta E_{s\text{–}t}$
1$_s$, **1**$_t$	33.00	**13**$_s$, **13**$_t$	12.39
2$_s$, **2**$_t$	23.40	**14**$_s$, **14**$_t$	19.43
3$_s$, **3**$_t$	31.40	**15**$_s$, **15**$_t$	16.50
4$_s$, **4**$_t$	17.53	**16**$_s$, **16**$_t$	13.44
5$_s$, **5**$_t$	21.86	**17**$_s$, **17**$_t$	16.02
6$_s$, **6**$_t$	22.07	**18**$_s$, **18**$_t$	16.45
7$_s$, **7**$_t$	31.43	**19**$_s$, **19**$_t$	20.44
8$_s$, **8**$_t$	29.22	**20**$_s$, **20**$_t$	20.10
9$_s$, **9**$_t$	39.75	**21**$_s$, **21**$_t$	30.53
10$_s$, **10**$_t$	21.95	**22**$_s$, **22**$_t$	20.33
11$_s$, **11**$_t$	21.47	**23**$_s$, **23**$_t$	14.50
12$_s$, **12**$_t$	30.02	**24**$_s$, **24**$_t$	14.46

Table 3 Calculated second-order perturbation stabilization energies ($E^{(2)}$), for the intermolecular interactions (donor/acceptor NBO) of singlet silylenes, at the B3LYP/6–311++G** level of theory

Silylenes	Donor→acceptor	$E^{(2)}$ (kcal/mol)
1$_s$	-	-
2$_s$	-	-
3$_s$	$\sigma_{C(A)\text{-}Si(B)} \rightarrow LP^*_{\ddot{S}i}$	5.16
4$_s$	-	-
5$_s$	$\sigma_{Si(A)\text{-}Si(B)} \rightarrow LP^*_{\ddot{S}i}$	4.25
6$_s$	$\sigma_{C(D)\text{-}Si(C)} \rightarrow LP^*_{\ddot{S}i}$	4.85
7$_s$	$\sigma_{C(A)\text{-}Si(F) \text{ and } C(A)\text{-}Si(B)} \rightarrow LP^*_{\ddot{S}i}$	4.36
8$_s$	$\sigma_{C(D)\text{-}Si(C) \text{ and } C(A)\text{-}Si(F)} \rightarrow LP^*_{\ddot{S}i}$	3.35
9$_s$	$\sigma_{C(A)\text{-}Si(B) \text{ and } C(D)\text{-}Si(C)} \rightarrow LP^*_{\ddot{S}i}$	5.23
10$_s$	$\sigma_{C(A)\text{-}Si(B) \text{ and } C(A)\text{-}Si(F)} \rightarrow LP^*_{\ddot{S}i}$	4.20
11$_s$	$\sigma_{Si(A)\text{-}Si(B)} \rightarrow LP^*_{\ddot{S}i}$	3.35
12$_s$	$\sigma_{C(A)\text{-}Si(F)} \rightarrow LP^*_{\ddot{S}i}$	3.52
	$\sigma_{C(A)\text{-}Si(B)} \rightarrow LP^*_{\ddot{S}i}$	2.97
	$\sigma_{C(D)\text{-}Si(E)} \rightarrow LP^*_{\ddot{S}i}$	3.54
13$_s$	$\sigma_{Si(A)\text{-}Si(B) \text{ and } Si(A)\text{-}Si(F)} \rightarrow LP^*_{\ddot{S}i}$	1.24
14$_s$	$\sigma_{Si(A)\text{-}Si(B)} \rightarrow LP^*_{\ddot{S}i}$	2.44
	$\sigma_{C(D)\text{-}Si(E)} \rightarrow LP^*_{\ddot{S}i}$	2.87
15$_s$	$\sigma_{Si(A)\text{-}Si(B)} \rightarrow LP^*_{\ddot{S}i}$	3.75
16$_s$	$\sigma_{Si(A)\text{-}Si(B) \text{ and } Si(D)\text{-}Si(E)} \rightarrow LP^*_{\ddot{S}i}$	1.67
17$_s$	$\sigma_{Si(A)\text{-}Si(B) \text{ and } Si(A)\text{-}Si(F)} \rightarrow LP^*_{\ddot{S}i}$	2.68
18$_s$	$\sigma_{Si(A)\text{-}Si(B)} \rightarrow LP^*_{\ddot{S}i}$	4.47
	$\sigma_{Si(C)\text{-}Si(D)} \rightarrow LP^*_{\ddot{S}i}$	2.82
19$_s$	$\sigma_{Si(C)\text{-}C(D)} \rightarrow LP^*_{\ddot{S}i}$	4.61
	$\sigma_{C(D)\text{-}Si(E)} \rightarrow LP^*_{\ddot{S}i}$	3.12
20$_s$	$\sigma_{Si(A)\text{-}Si(B)} \rightarrow LP^*_{\ddot{S}i}$	2.45
	$\sigma_{C(D)\text{-}Si(C)} \rightarrow LP^*_{\ddot{S}i}$	4.20
21$_s$	$\sigma_{C(A)\text{-}Si(B) \text{ and } C(D)\text{-}Si(E)} \rightarrow LP^*_{\ddot{S}i}$	3.29
	$\sigma_{C(D)\text{-}Si(C) \text{ and } C(A)\text{-}Si(F)} \rightarrow LP^*_{\ddot{S}i}$	3.37
22$_s$	$\sigma_{Si(A)\text{-}Si(B) \text{ and } Si(A)\text{-}Si(F)} \rightarrow LP^*_{\ddot{S}i}$	1.29
	$\sigma_{C(D)\text{-}Si(E) \text{ and } Si(C)\text{-}C(D)} \rightarrow LP^*_{\ddot{S}i}$	3.57
23$_s$	$\sigma_{Si(A)\text{-}Si(B)} \rightarrow LP^*_{\ddot{S}i}$	2.86
	$\sigma_{Si(D)\text{-}Si(C) \text{ and } Si(F)\text{-}Si(A)} \rightarrow LP^*_{\ddot{S}i}$	1.49
24$_s$	$\sigma_{Si(A)\text{-}Si(B) \text{ and } Si(D)\text{-}Si(E)} \rightarrow LP^*_{\ddot{S}i}$	1.94
	$\sigma_{C(A)\text{-}Si(F) \text{ and } Si(C)\text{-}C(D)} \rightarrow LP^*_{\ddot{S}i}$	1.47

Table 4 The highest occupied and the lowest unoccupied molecular orbital energies (E_{HOMO}/eV, E_{LUMO}/eV, respectively), along with band gaps ($\Delta E_{HOMO-LUMO}$, kcal/mol), nucleophilicity (N), chemical potential (μ), proton affinity (ΔE_{PA}, kcal/mol), zero-point vibrational energy (ZPVE, kcal/mol), and global electrophilicity (ω) for singlet silylenes (**1**$_s$-**24**$_s$), at B3LYP/6–311++G** level of theory

Silylenes	E_{HOMO}	E_{LUMO}	$\Delta E_{HOMO-LUMO}$	N (eV)	ω (eV)	μ (eV)	η (eV)	ΔE_{PA}[a]	ZPVE
1$_s$	−5.91	−2.49	78.67	3.55	2.58	−4.20	3.41	−216.20	91.94
2$_s$	−6.39	−2.93	79.95	3.06	3.13	−4.66	3.47	−222.65	86.26
3$_s$	−5.92	−2.59	77.00	3.53	2.71	−4.25	3.34	−219.79	84.63
4$_s$	−6.07	−3.32	63.56	3.38	4.00	−4.69	2.76	−218.66	80.55
5$_s$	−5.85	−3.04	64.88	3.60	3.51	−4.44	2.81	−223.18	79.68
6$_s$	−5.80	−2.98	65.20	3.64	3.42	−4.40	2.83	−224.87	79.13
7$_s$	−5.96	−2.63	76.85	3.49	2.77	−4.30	3.33	−221.05	77.72
8$_s$	−5.93	−2.71	74.19	3.53	2.90	−4.32	3.22	−221.22	77.47
9$_s$	−5.98	−2.67	76.20	3.47	2.83	−4.33	3.30	−222.67	78.17
10$_s$	−5.81	−2.97	65.37	3.65	3.40	−4.39	2.83	−224.44	72.22
11$_s$	−5.90	−3.11	64.48	3.55	3.63	−4.50	2.80	−225.21	73.22
12$_s$	−6.01	−2.74	75.37	3.45	2.92	−4.37	3.27	−223.73	71.20
13$_s$	−5.91	−3.12	64.35	3.54	3.65	−4.51	2.79	−224.71	73.24
14$_s$	−5.81	−3.14	61.43	3.65	3.75	−4.47	2.66	−224.69	72.47
15$_s$	−6.07	−3.42	61.08	3.38	4.25	−4.75	2.66	−220.87	74.13
16$_s$	−6.04	−3.57	57.03	3.41	4.67	−4.80	2.47	−220.25	67.62
17$_s$	−6.07	−3.47	59.86	3.38	4.38	−4.77	2.60	−223.73	67.75
18$_s$	−6.16	−3.53	60.67	3.29	4.46	−4.84	2.63	−221.81	68.22
19$_s$	−5.87	−3.12	63.42	3.58	3.68	−4.50	2.75	−224.49	66.24
20$_s$	−5.92	−3.20	62.73	3.53	3.82	−4.56	2.72	−226.45	66.64
21$_s$	−6.08	−2.77	76.35	3.37	2.96	−4.43	3.31	−225.17	64.88
22$_s$	−5.98	−3.22	63.67	3.47	3.83	−4.60	2.76	−224.76	60.33
23$_s$	−6.13	−3.61	57.96	3.32	4.72	−4.87	2.51	−222.48	61.73
24$_s$	−6.17	−3.71	56.88	3.28	4.94	−4.94	2.47	−223.96	55.83

[a] Based on the reaction: $R_1R_2Si: + H^+ \rightarrow R_1R_2Si^+H$

Table 5 NBO charges on -S̈i- for singlet (**1**$_s$–**24**$_s$) and triplet (**1**$_t$–**24**$_t$) silylenes, at B3LYP/6–311++G** level of theory

Silylenes	S̈i	Silylenes	S̈i	Silylenes	S̈i	Silylenes	S̈i
1$_s$	1.001	**1**$_t$	0.7605	**13**$_s$	0.7207	**13**$_t$	0.4861
2$_s$	0.6589	**2**$_t$	0.4195	**14**$_s$	0.7175	**14**$_t$	0.4643
3$_s$	1.0168	**3**$_t$	0.7879	**15**$_s$	0.2966	**15**$_t$	0.0773
4$_s$	0.2789	**4**$_t$	0.0592	**16**$_s$	0.3319	**16**$_t$	0.0866
5$_s$	0.6884	**5**$_t$	0.4531	**17**$_s$	0.3154	**17**$_t$	0.0967
6$_s$	0.6788	**6**$_t$	0.4418	**18**$_s$	0.3200	**18**$_t$	0.1082
7$_s$	1.0341	**7**$_t$	0.8085	**19**$_s$	0.7353	**19**$_t$	0.4937
8$_s$	1.0449	**8**$_t$	0.8080	**20**$_s$	0.7451	**20**$_t$	0.5075
9$_s$	1.0316	**9**$_t$	0.8352	**21**$_s$	1.0857	**21**$_t$	0.8872
10$_s$	0.6938	**10**$_t$	0.4584	**22**$_s$	0.7774	**22**$_t$	0.5291
11$_s$	0.7056	**11**$_t$	0.4844	**23**$_s$	0.3529	**23**$_t$	0.1234
12$_s$	1.0608	**12**$_t$	0.8524	**24**$_s$	0.3827	**24**$_t$	0.1545

stability than **6** with $\sigma_{C(D)\text{-}Si(C)} \rightarrow LP^{*}_{Si}$ interaction ($E^{(2)}$ = 4.85 kcal/mol). Likewise, silylene **19** with high interactions ($\sigma_{Si(C)\text{-}C(D)} \rightarrow LP^{*}_{Si}$, $E^{(2)}$ = 4.61 kcal/mol) has lower stability than **11** with $\sigma_{Si(A)\text{-}Si(B)} \rightarrow LP^{*}_{Si}$ interaction ($E^{(2)}$ = 3.35 kcal/mol). Silylene **10** with two interactions ($\sigma_{C(A)\text{-}Si(B) \text{ and } C(A)\text{-}Si(F)} \rightarrow LP^{*}_{Si}$, $E^{(2)}$ = 4.20 kcal/mol) has higher stability then **5** with $\sigma_{C(D)\text{-}Si(C)} \rightarrow LP^{*}_{Si}$ interaction ($E^{(2)}$ = 4.85 kcal/mol) (Table 3).

In order to characterize the substituent effect on stability data, we have compared and contrasted the zero-point vibrational energy (ZPVE) of singlet silylenes. Interestingly, the effect of successive divalent Si substituting on the calculated ZPVE shows the addition of silicon atoms decreases ZPVE. For example, silylene **23**$_s$ with six silicon atoms has low stability (ΔE_{s-t} = 14.50 kcal/mol) and ZPVE (55.83 kcal/mol). Likewise, bicyclo[2.2.1]heptanylene (**1**$_s$) without any silicon has high stability (ΔE_{s-t} = 33.00 kcal/mol) and ZPVE (93.71 kcal/mol) (Table 4).

The correlation coefficients of the fit between the band gaps ($\Delta E_{HOMO-LUMO}$) of our silylenes with $\Delta E_{s\text{-}t}$ and E_{LOMO} are 0.78 and 0.84, respectively. For instance, silylene **9**$_s$ has high $\Delta E_{s\text{-}t}$ (39.75 kcal/mol), $\Delta E_{HOMO-LUMO}$ (76.20 kcal/mol), and E_{LOMO} (−2.67 eV) (Fig. 1 (a and b) and Table 4). Furthermore, the direct relationship between the ΔE_{s-t} with μ and η are demonstrated by the correlation coefficient of the linear fit between the two values (R^2 = 0.65 and 0.77, respectively). For example, silylene **1**$_s$ has high stability (ΔE_{s-t} = 33 kcal/mol), μ (−4.20 eV), and η (3.41 eV) (Fig. 1 (c and d)).

Also, the ω appears inverse correlation with our results of ΔE_{s-t} and $\Delta E_{HOMO-LUMO}$ values (R^2 = 0.86 and 0.78, respectively) (Fig. 1 (e and f)). The increasing electropositive or π-acceptor capability of the substituents decreases the

Table 6 Calculated second-order perturbation stabilization energies ($E^{(2)}$), for the intermolecular interactions (donor/acceptor NBO) and bond angle (deg) of singlet (**1'**$_s$-**24'**$_s$) protonated silylenes, at the B3LYP/6–311++G** level of theory

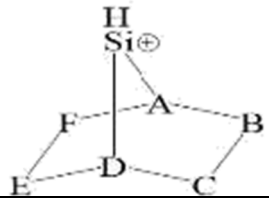

Protonated silylenes	Donor→Acceptor	$E^{(2)}$ (kcal/mol)	Bond angle (deg)	
			∠SiDC	∠SiAB
 **1'**$_s$	$\sigma_{C(D)\text{-}C(C)} \rightarrow LP^{*}_{Si\text{-}H}$ $\sigma_{C(A)\text{-}C(B)} \rightarrow LP^{*}_{Si\text{-}H}$ $\sigma_{C(B)\text{-}C(C)} \rightarrow LP^{*}_{Si\text{-}H}$	9.93 10.34 3.66	91.62	91.26
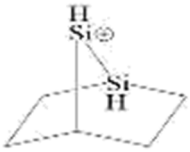 **2'**$_s$	$\sigma_{C(D)\text{-}C(E)} \rightarrow LP^{*}_{Si\text{-}H}$ $\sigma_{Si(A)\text{-}C(F)} \rightarrow LP^{*}_{Si\text{-}H}$ $\sigma_{C(E)\text{-}C(F)} \rightarrow LP^{*}_{Si\text{-}H}$ $\sigma_{C(D)\text{-}SiH} \rightarrow LP^{*}_{Si\text{-}H}$ $\sigma_{C(E)\text{-}H(exo)} \rightarrow LP^{*}_{Si\text{-}H}$	21.27 2.08 1.54 3.15 33.49	114.98	88.84
 **3'**$_s$	$\sigma_{C(D)\text{-}C(C)} \rightarrow LP^{*}_{Si\text{-}H}$ $\sigma_{Si(A)\text{-}C(B)} \rightarrow LP^{*}_{Si\text{-}H}$ $\sigma_{C(C)\text{-}Si(B)} \rightarrow LP^{*}_{Si\text{-}H}$	6.31 26.55 4.15	97.84	93.10
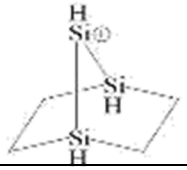	$\sigma_{Si(A)\text{-}C(F) \text{ and } C(D)\text{-}Si(C)} \rightarrow LP^{*}_{Si\text{-}H}$	1.52	103.12	99.04

Table 6 (continued)

4′s				
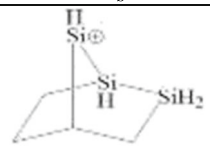 **5′s**	$\sigma_{C(D)-C(C)} \rightarrow LP^{*}_{Si-H}$ $\sigma_{Si(A)-Si(B)} \rightarrow LP^{*}_{Si-H}$ $\sigma_{C(C)-Si(B)} \rightarrow LP^{*}_{Si-H}$	5.63 21.45 3.27	101.11	81.13
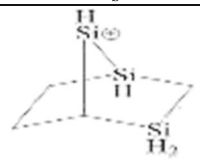 **6′s**	$\sigma_{C(D)-C(C)} \rightarrow LP^{*}_{Si-H}$ $\sigma_{Si(A)-C(B)} \rightarrow LP^{*}_{Si-H}$ $\sigma_{Si(C)-C(B)} \rightarrow LP^{*}_{Si-H}$ $\sigma_{C(D)-SiH} \rightarrow LP^{*}_{Si-H}$	31.82 1.80 1.15 1.30	94.08	94.24
 **7′s**	$\sigma_{C(D)-C(C)}$ and $C(D)-C(E) \rightarrow LP^{*}_{Si-H}$ $\sigma_{C(A)-Si(F)}$ and $C(A)-Si(B) \rightarrow LP^{*}_{Si-H}$ $\sigma_{C(C)-Si(B)}$ and $Si(F)-C(E) \rightarrow LP^{*}_{Si-H}$	1.95 9.78 1.43	101.56	98.29
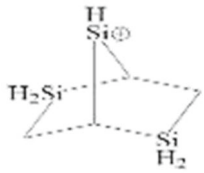 **8′s**	$\sigma_{C(D)-Si(C)}$ and $C(A)-Si(F) \rightarrow LP^{*}_{Si-H}$ $\sigma_{C(D)-C(E)}$ and $C(A)-C(B) \rightarrow LP^{*}_{Si-H}$ $\sigma_{Si(C)-C(B)}$ and $Si(F)-C(E) \rightarrow LP^{*}_{Si-H}$	8.93 2.64 1.42	97.22	102.94
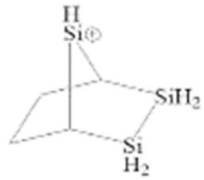 **9′s**	$\sigma_{C(D)-Si(C)}$ and $C(A)-Si(B) \rightarrow LP^{*}_{Si-H}$ $\sigma_{Si(C)-Si(B)} \rightarrow LP^{*}_{Si-H}$	20.74 7.38	97.37	97.37
 **10′s**	$\sigma_{C(A)-Si(B)}$ and $C(A)-Si(F) \rightarrow LP^{*}_{Si-H}$	8.58	92.17	104.43
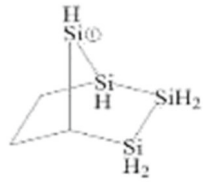 **11′s**	$\sigma_{C(D)-Si(C)} \rightarrow LP^{*}_{Si-H}$ $\sigma_{Si(A)-Si(B)} \rightarrow LP^{*}_{Si-H}$ $\sigma_{Si(C)-Si(B)} \rightarrow LP^{*}_{Si-H}$ $\sigma_{C(D)-SiH} \rightarrow LP^{*}_{Si-H}$	28.13 6.16 3.33 1.15	97.48	91.10
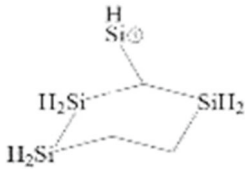 **12′s**	$\sigma_{C(A)-Si(B)} \rightarrow LP^{*}_{Si-H}$ $\sigma_{C(A)-Si(F)} \rightarrow LP^{*}_{Si-H}$ $\sigma_{Si(F)-Si(E)} \rightarrow LP^{*}_{Si-H}$ $\sigma_{C(D)-Si(E)} \rightarrow LP^{*}_{Si-H}$	2.50 15.86 6.36 15.90	105.79	100.88

Table 6 (continued)

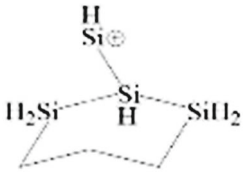 **13′$_s$**	$\sigma_{C(D)-C(C)} \rightarrow LP^*_{Si-H}$ $\sigma_{Si(A)-Si(F)} \rightarrow LP^*_{Si-H}$ $\sigma_{C(C)-Si(B)} \rightarrow LP^*_{Si-H}$ $\sigma_{Si(A)-Si(B)} \rightarrow LP^*_{Si-H}$	3.67 2.79 2.18 14.35	102.60	82.91
 **14′$_s$**	$\sigma_{C(D)-Si(E)} \rightarrow LP^*_{Si-H}$ $\sigma_{Si(A)-Si(B)} \rightarrow LP^*_{Si-H}$ $\sigma_{Si(A)-C(F)} \rightarrow LP^*_{Si-H}$ $\sigma_{C(F)-Si(E)} \rightarrow LP^*_{Si-H}$	22.51 1.07 3.01 1.73	113.53	87.73
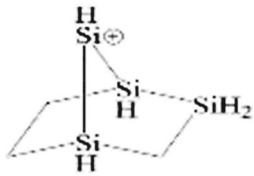 **15′$_s$**	$\sigma_{Si(D)-C(C)} \rightarrow LP^*_{Si-H}$ $\sigma_{Si(A)-Si(B)} \rightarrow LP^*_{Si-H}$ $\sigma_{C(C)-Si(B)} \rightarrow LP^*_{Si-H}$ $\sigma_{Si(A)-SiH} \rightarrow LP^*_{Si-H}$	2.89 27.94 1.29 1.33	97.93	82.20
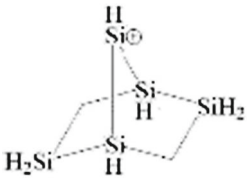 **16′$_s$**	$\sigma_{Si(A)-Si(B)} \rightarrow LP^*_{Si-H}$ $\sigma_{Si(D)-Si(E)} \rightarrow LP^*_{Si-H}$	4.65 4.65	100.89	86.55
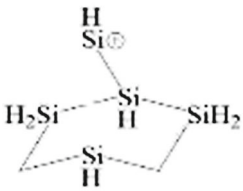 **17′$_s$**	$\sigma_{Si(D)-C(C)} \rightarrow LP^*_{Si-H}$ $\sigma_{Si(A)-Si(B)} \rightarrow LP^*_{Si-H}$ $\sigma_{C(C)-Si(B)} \rightarrow LP^*_{Si-H}$ $\sigma_{Si(A)-SiH} \rightarrow LP^*_{Si-H}$	1.81 53.63 1.49 2.56	98.29	75.07
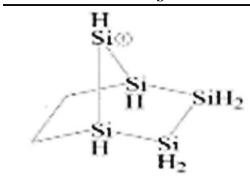 **18′$_s$**	$\sigma_{Si(D)-Si(C)} \rightarrow LP^*_{Si-H}$ $\sigma_{Si(A)-Si(B)} \rightarrow LP^*_{Si-H}$ $\sigma_{Si(C)-Si(B)} \rightarrow LP^*_{Si-H}$	7.43 14.27 1.88	93.97	89.96
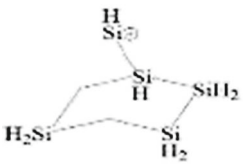 **19′$_s$**	$\sigma_{C(D)-Si(C)} \rightarrow LP^*_{Si-H}$ $\sigma_{Si(A)-Si(B)} \rightarrow LP^*_{Si-H}$ $\sigma_{Si(C)-Si(B)} \rightarrow LP^*_{Si-H}$ $\sigma_{C(D)-Si(E)} \rightarrow LP^*_{Si-H}$	11.87 2.69 1.60 4.80	104.71	90.59
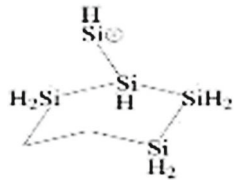 **20′$_s$**	$\sigma_{Si(D)-Si(C)} \rightarrow LP^*_{Si-H}$ $\sigma_{Si(A)-Si(B)} \rightarrow LP^*_{Si-H}$ $\sigma_{Si(C)-Si(B)} \rightarrow LP^*_{Si-H}$	20.25 12.36 6.34	98.90	86.07

Table 6 (continued)

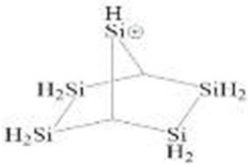 **21′$_s$**	$\sigma_{C(D)-Si(C)}$ and $C(A)-Si(F) \rightarrow LP^*_{Si-H}$ $\sigma_{C(A)-Si(B)}$ and $C(D)-Si(E) \rightarrow LP^*_{Si-H}$ $\sigma_{Si(C)-Si(B)}$ and $Si(E)-Si(F) \rightarrow LP^*_{Si-H}$	7.78 7.51 2.82	102.64	102.97
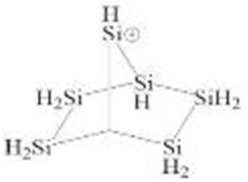 **22′$_s$**	$\sigma_{C(D)-Si(C)}$ and $C(D)-Si(E) \rightarrow LP^*_{Si-H}$ $\sigma_{Si(A)-Si(B)}$ and $Si(A)-Si(F) \rightarrow LP^*_{Si-H}$ $\sigma_{Si(C)-Si(B)}$ and $Si(F)-Si(E) \rightarrow LP^*_{Si-H}$	7.49 2.56 1.45	107.23	90.03
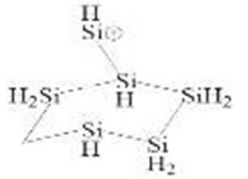 **23′$_s$**	$\sigma_{Si(D)-Si(C)} \rightarrow LP^*_{Si-H}$ $\sigma_{Si(A)-Si(B)} \rightarrow LP^*_{Si-H}$ $\sigma_{Si(C)-Si(B)} \rightarrow LP^*_{Si-H}$ $\sigma_{Si(A)-Si(F)} \rightarrow LP^*_{Si-H}$	3.28 12.11 1.17 1.91	94.36	91.88
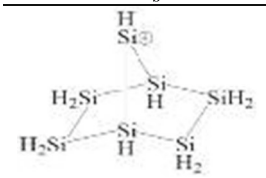 **24′$_s$**	$\sigma_{Si(D)-Si(C)}$ and $Si(D)-Si(F) \rightarrow LP^*_{Si-H}$ $\sigma_{Si(A)-Si(B)}$ and $Si(D)-Si(E) \rightarrow LP^*_{Si-H}$	4.05 4.47	97.19	96.27

population of the Si $3p_z$ orbital leading to a high positive electrostatic potential in the lone pair region yielding higher electrophilicity of the silicon atom, thereby increasing the stability of the triplet silylene and decreasing singlet-triplet gap [44, 45]. In other words, μ is a measure of stability; therefore, as μ becomes high negative, the structure becomes less stable and easy to get an electron. For instance, **24$_s$** with the highest μ (−4.94 eV) and ω (4.94 eV) has low stability (ΔE_{s-t} = 14.46 kcal/mol) and band gap ($\Delta E_{HOMO-LUMO}$ = 56.88 kcal/mol). On the other extreme, **1$_s$** with the lowest negative μ (−54.29 eV) and ω (2.58 eV) shows high stability (ΔE_{s-t} = 33.00 kcal/mol) and band gap ($\Delta E_{HOMO-LUMO}$ = 78.87 kcal/mol) (Tables 2 and 4).

The nucleophilicity index and gas-phase proton affinity (PA) are critical factors for showing the aptitude of our silylenes for coordination to transition metal complexes. As a result, silylene **12$_s$** with rather high stability (ΔE_{s-t} = 30.02 kcal/mol) and N (3.45 eV) has high negative ΔE_{PA} (−223.73 kcal/mol) that can be applied as accumulated multidentate ligands (Tables 2 and 4).

The electrostatic potential (ESP) map has largely been used as a molecular descriptor of the chemical reactivity, which takes part in both electrophilic and nucleophilic reactions. For investigating, the electrostatic potential (ESP) surfaces are plotted over the optimized electronic structures of our silylenes using density functional B3LYP method with 6–311++G** basis set. The red and blue regions indicate the lowest (most negative) and highest (most positive) electrostatic potential energy values, respectively (Fig. 2) [46]. The ESP maps show that silylene center with red region has the negative potential as a nucleophilicity site.

The NBO charges on –S̈i– were computed for the singlet and triplet states of the silylene species (Table 5). Charges on all the triplet silylenes are less than those of their corresponding singlet species. For example, atomic charges on –S̈i– of **2$_s$** and **2$_t$** are +0.6589 and + 0.4195, receptively. Due to the rather higher electronegativity of carbon than silicon atom, it is anticipated to place a higher partial positive atomic charge on its adjacent silylene (–S̈i–). In the other words, silicon atoms in singlets tend to have their nonbonding electrons in the atomic orbitals with higher *s*-character. Consequently, electropositive substitutions (–S̈i–) transfer charge from their corresponding S̈i–A and S̈i–D bonding orbitals with higher *p*-character to the partially populated *s*-type orbital on the silicon atom. For

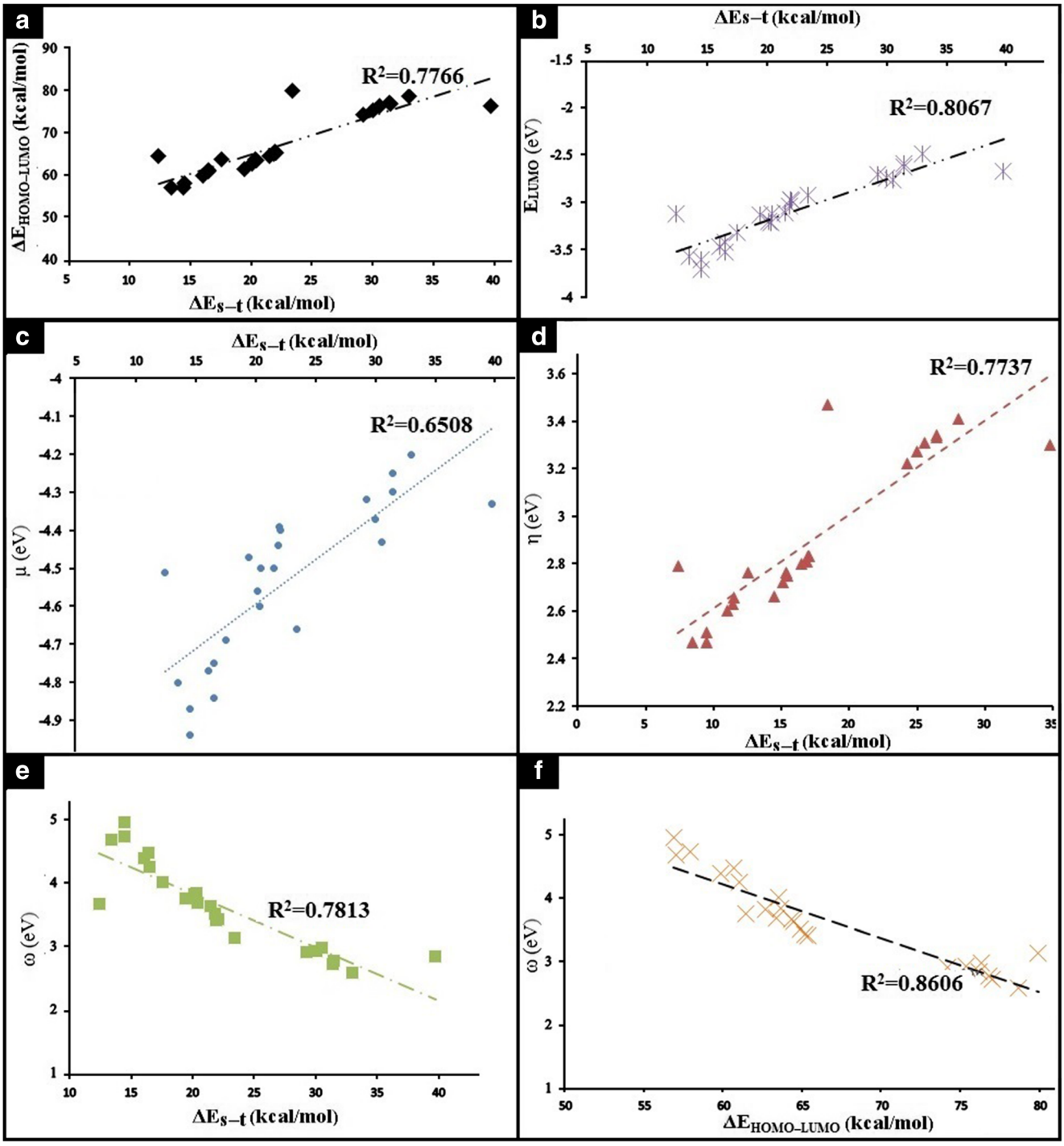

Fig. 1 Correlation diagrams between $\Delta E_{HOMO-LUMO}$ (kcal/mol) and ΔE_{s-t} (kcal/mol) (**a**), E_{LUMO} (eV) and ΔE_{s-t} (kcal/mol) (**b**), μ (eV) and ΔE_{s-t} (kcal/mol) (**c**), η (eV), and ΔE_{s-t} (kcal/mol) (d), ω (eV) and ΔE_{s-t} (kcal/mol), and ω (eV) and $\Delta E_{HOMO-LUMO}$ (kcal/mol) (**d**)

example, $\mathbf{3}_s$ with two carbons adjacent to its silylene center has a more positive atomic charge on its –S̈i– (+1.0168) than $\mathbf{2}_s$ which has one nitrogen (–S̈i– = +0.6589).

The gas-phase proton affinity (PA) is one of the most important thermodynamic properties that shows the importance of acid-base chemistry [47]. The ΔE_{PA} of reactions for singlet silylenes is calculated, at B3LYP/6–311++G** levels of theory. We have employed the NBO analysis to stress the roles of intermolecular orbital interactions through second-order perturbation theory. The NBO analysis provides significant

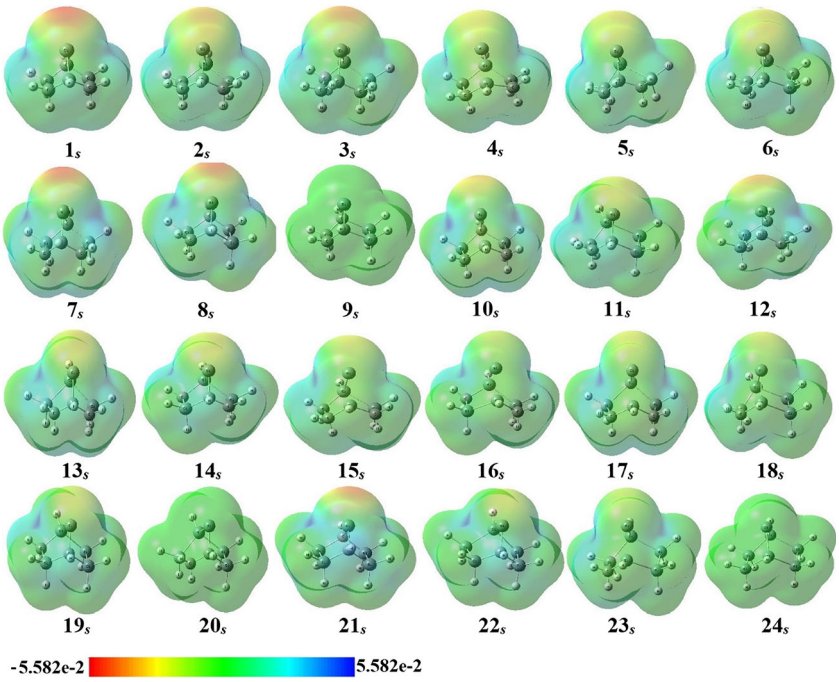

Fig. 2 The ESP maps of singlet ($\mathbf{1}_s$–$\mathbf{24}_s$) silylenes, at B3LYP/6–311++G** level of theory

evidence for the nature of our protonated silylenes. Every interaction that stabilization of positive charge causes increased negative ΔE_{PA}. In this regard, silylene $\mathbf{1_s}$ without any silicon atom at its structure has the lowest ΔE_{PA} (−216.20 kcal/mol). Silicon atoms at A and D situations have less effect on the stability of the positive center. For instance, silylene $\mathbf{3}_s$ with one Si at B situation has higher ΔE_{PA} than $\mathbf{4}_s$ with two Si at A and D situations because protonated silylene $\mathbf{3'}_s$ has higher $\sigma_{(A)\text{-}(B)} \rightarrow LP^*_{Si\text{-}H}$ interaction ($E^{(2)}$ = 26.55 kcal/mol) than $\mathbf{4'}_s$ ($E^{(2)}$ = 0.76 kcal/mol).

Contrary to our anticipation, silylene $\mathbf{2}_s$ with one silicon at situation A has the rather high ΔE_{PA} (−222.65 kcal/mol) because of high $\sigma_{C(E)\text{-}H(exo)} \rightarrow LP^*_{Si\text{-}H}$ interactions (33.49 kcal/mol) at $\mathbf{2'}_s$ (Tables 4 and 6). The silicon atoms in the B situation are better than C for stabilizing the positive center of silylene. For example, silylene $\mathbf{7}_s$ has higher ΔE_{PA} than $\mathbf{8}_s$ (−221.05 and − 221.22 kcal/mol, respectively), because protonated silylene $\mathbf{7'}_s$ has higher $\sigma_{C(A)\text{-}Si(B)} \rightarrow LP^*_{Si\text{-}H}$ interaction ($E^{(2)}$ = 9.78 kcal/mol) than $\sigma_{C(D)\text{-}Si(C)} \rightarrow LP^*_{Si\text{-}H}$ interaction ($E^{(2)}$ = 8.93 kcal/mol) of $\mathbf{8'}_s$. The important factor for stability of protonated silylenes is their bond angles (∠SiDC and ∠SiAB). For instance, the protonated center of $\mathbf{17'}_s$ has stabilized its positive charge by bending too much to one side (∠SiAB = 75.07°), so it has the highest $\sigma_{Si(A)\text{-}Si(B)} \rightarrow LP^*_{Si\text{-}H}$ interactions ($E^{(2)}$ = 53.63 kcal/mol). Likewise, silylenes $\mathbf{11}_s$ and $\mathbf{20}_s$ with high interactions and low bond angles (∠SiDC and ∠SiAB) have the highest ΔE_{PA} (−225.21 and − 226.45 kcal/mol, respectively) (Tables 4 and 6).

Conclusions

In this research, we have studied thermodynamical and geometrical parameters of novel singlet (s) and triplet (t) forms of bicyclo[2.2.1]hepta-7-silylenes, all of which appear as minima on their potential energy surfaces at B3LYP/6–311++G** level of theory. The 2,3-disilabicyclo[2.2.1]hepta-7-silylene (**9**) shows the highest stability indicated by its relatively high $\Delta E_{s\text{-}t}$. The overall trend of $\Delta E_{s\text{-}t}$ is **9 > 1 > 7 > 3 > 21 > 12 > 8 > 2 > 6 > 10 > 5 > 11 > 19 > 22 > 20 > 14 > 4 > 15 > 18 > 17 > 23 > 24 > 16 > 13**, which appears rather similar to the trend of $\Delta E_{HOMO\text{-}LUMO}$ and E_{LOMO}. Silylenes **3**, **7**, **8**, **9**, **12**, and **21** with β-silicon have higher stability for $\sigma_{C\text{-}Si} \rightarrow LP^*_{Si}$ interactions than others. So, silylene **9** has the highest stability for two $\sigma_{C(A)\text{-}Si(B)\ \text{and}\ Si(C)\text{-}C(D)} \rightarrow LP^*_{Si}$ interactions with the highest $E^{(2)}$ (5.23 kcal/mol).

The electrophilicity (ω) appears inverse correlation with our results of $\Delta E_{s\text{–}t}$ and $\Delta E_{HOMO\text{–}LUMO}$ values (R^2 = 0.86 and 0.78, respectively). Silylene $\mathbf{1}_s$ has a high stability ($\Delta E_{s\text{–}t}$ = 33.00 kcal/mol), $\Delta E_{HOMO\text{-}LUMO}$ (78.67 kcal/mol), η (3.41), and NBO charge on -S̈i- (1.001) has low ΔE_{PA} (−216.20 kcal/mol), negative μ (−4.20 eV), and ω (2.58 eV). The interactions of donor and acceptor NBOs give a detailed assessment of ΔE_{PA} and geometrical features of our protonated silylenes. Contrary to our anticipation, 1-silabicyclo[2.2.1]hepta-7-silylene ($\mathbf{2_s}$) with one silicon has the rather high ΔE_{PA} (−222.65 kcal/mol) because of high $\sigma_{C(E)\text{-}H(exo)} \rightarrow LP^*_{Si\text{-}H}$ interactions (33.49 kcal/mol) at protonated silylene $\mathbf{2'_s}$. Also, the 2,6-disilabicyclo[2.2.1]hepta-7-silylene ($\mathbf{7}_s$) has higher ΔE_{PA} than 3,6-

disilabicyclo[2.2.1]hepta-7-silylene (**8**$_s$) (−221.05 and −221.22 kcal/mol, respectively), because protonated silylene **7'**$_s$ has higher $\sigma_{C(A)\text{-}Si(B)} \rightarrow LP^*_{Si\text{-}H}$ interaction ($E^{(2)}$ = 9.78 kcal/mol) than $\sigma_{C(D)\text{-}Si(C)} \rightarrow LP^*_{Si\text{-}H}$ interaction ($E^{(2)}$ = 8.93 kcal/mol) of **8'**$_s$.

The nucleophilicity index and gas-phase proton affinity (PA) are crucial factors for showing the aptitude of our silylenes for coordination to transition metal complexes. As a result, we introduce silylene **12**$_s$ with rather high stability ($\Delta E_{s\text{-}t}$ = 30.02 kcal/mol), N (3.45 eV), and negative ΔE_{PA} (−223.73 kcal/mol) that can be applied as accumulated multidentate ligands.

Supplementary Information The online version contains supplementary material available at https://doi.org/10.1007/s00894-021-04726-z.

Acknowledgements We acknowledge the support from the Tarbiat Modares University (TMU).

Availability of data and material Not applicable.

Code availability Not applicable.

Declaration

Conflict of interest There authors declare no competing interests.

References

1. Ashenagar S, Kassaee MZ (2018). Turk. J. Chem. 42(4):974–987
2. Schoeller WW, Sundermann A, Reiher M (1999). Inorg. Chem. 38: 29–37
3. Becerra R, Walsh R (2010). Dalt. Trans. 39:9217–9228
4. Mizuhata Y, Sasamori T, Tokitoh N (2009). Chem. Rev. 109: 3479–3511
5. Tokitoh N, Okazaki R (2000). Coord. Chem. Rev. 210:251–277
6. Bourissou D, Guerret O, Gabbai FP, Bertrand G (2000). Chem. Rev. 100:39–92
7. Barden CJ, Schaefer HF (2000). J. Chem. Phys. 112:6515–6516
8. Lee EPF, Dyke JM, Wright TG (2000). Chem. Phys. Lett. 326: 143–150
9. Bruce M (1991). Chem. Rev. 91:197–257
10. Ayoubi-Chianeh M, Kassaee MZ (2019). Res. Chem. Intermed. 45: 4677–4691
11. Haaf M, Schmedake TA, West R (2000). Acc. Chem. Res. 33:704–714
12. Yao S, Xiong Y, Driess M (2011). Organometallics 30:1748–1767
13. Blom B, Stoelzel M, Driess M (2013). Chem. Eur. J. 19:40
14. Goldberg DE, Harris DH, Lappert MF, Thomas KM (1976). J. Chem. Soc. Chem. Commun.:261
15. Abedini N, Kassaee MZ, Cummings PT (2020) Borasilylenes in focus: topological effects of nitrogen atoms by DFT. Silicon:1–7
16. Heaven MW, Metha GF, Buntine MA, Phys J (2001). Chem. A 105:1185–1196
17. Zachariah MR, Tsang W (1995). J. Phys. Chem. 99:5308–5318
18. Lucas DJ, Curtiss LA, Pople JA (1993). J. Chem. Phys. 99:6697–6703
19. Boudjouk P, Black E, Kumarathasan R (1991). Organometal. 10: 2095–2096
20. Kassaee MZ, Buazar F, Soleimani-Amiri S, Mol J (2008) Struct. THEOCHEM 866:52–57
21. Cote DR, Van Nguyen S, Stamper AK, Armbrust DS, Tobben D, Conti RA, Lee GY (1999) IBM J. res. Dev. 43:5–38
22. Kassaee MZ, Najafi Z, Shakib FA, Momeni MR (2011). J. Organometal. Chem. 696:2059–2064
23. Tamao K, Kobayashi M, Matsuo T, Furukawa S, Tsuji H (2012). Chem. Commun. 48:1030–1032
24. Holthausen MC, Koch W, Apeloig Y (1999). J. Am. Chem. Soc. 121:2623–2624
25. Kassaee MZ, Zandi H (2012). J. Phys. Org. Chem. 25:50–57
26. Sekiguchi A, Tanaka T, Ichinohe M, Akiyama K, Tero-Kubota S, Am J (2003). Chem. Soc. 125:4962–4963
27. West R, Fink MJ, Michl J (1981). Science 214:1343–1344
28. B. T. Luke, J. A. Pople, M-B. Krogh-Jespersen, Y. Apeloig, M. Karni, J. Am. Chem. Soc. 1986, 108, 270–284
29. Kalcher J, Sax AF, Mol J (1992) Struct. THEOCHEM 253:287–302
30. Krogh-Jespersen K (1985). J. Am. Chem. Soc. 107:537–543
31. Yoshida M, Tamaoki N (2002). Organometallics 21:2587–2589
32. Soleimani Purlak N, Kassaee MZ (2020). J. Phys. Org. Chem.: 33(6)
33. Yan Z, Truhlar DG (2008). Theor. Chem. Account 120:215–241
34. Becke AD (1988). Phys. Rev. 38:3098
35. Becke AD (1993). J. Chem. Phys. 98:5648–5652
36. Schmidt MW, Baldridge KK, Boatz JA, Elbert ST, Gordon MS, Jensen JH, Koseki S, Matsunaga N, Nguyen KA, Su S, Windus TL, Dupuis M, Montgomery JA (1993). J. Comput. Chem. 14:1347–1363
37. Kassaee MZ, Ashenagar S (2018). J. Mol. Model. 24:2–11
38. Domingo LR, Chamorro E, Perez P (2008). J. Org. Chem. 73: 4615–4624
39. Parr RG, Szentpaly L, Liu S (1999). J. Am. Chem. Soc. 121:1922–1924
40. Nyulaszi L, Belghazi A, Szetsi SK, Veszpremi T, Heinicke J (1994). THEOCHEM J. Mol. Struct. 313:73–81
41. Nyulaszi L, Schleyer PVR (1999). J. Am. Chem. Soc 121:6872–6875
42. Shimizu H, Gordon MS (1994). Organometallics 13:186–189
43. Lambert JB, Zhao Y (1996). J. Am. Chem. Soc. 118:7867–7868
44. J. Ola'h, T.Veszpre'mi, F. D. Proft, P. Geerlings, *J. Phys.* Chem. A 2007, 111, 10815–10823
45. J. Ola'h, F. De Proft, T.Veszpre'mi, P. Geerlings, *J. Phys.* Chem. A 2005, 109, 1608–1615
46. Scrocco E, Tomasi J (1973). New Concepts II 42:95–170
47. Parr RG, Pearson RG (1983). J. Am. Chem. Soc. 105:7512–7516